International Journal of Heat and Mass Transfer 52 (2009) 2914–2917

Contents lists available at ScienceDirect

International Journal of Heat and Mass Transfer

journal homepage: www.elsevier.com/locate/ijhmt

Technical Note

Simple two-layer model for temperature distribution in the inner part of turbulent boundary layers in adverse pressure gradients

Sedat F. Tardu*

Laboratoire des Ecoulements Géophysiques et Industriels (LEGI), B.P. 53 X 38041, Grenoble Cédex, France

ARTICLE INFO

Article history:
Received 4 July 2008
Received in revised form 13 November 2008
Available online 7 February 2009

Keywords:
Adverse pressure gradient
Turbulent boundary layers
One-point closure
Local self-similarity

ABSTRACT

A simple one-point closure for the inner region of turbulent boundary layers subjected to adverse pressure gradient is introduced. The use of local wall variables leads to self-similarity for the temperature distribution but not the velocity. A turbulent velocity scale directly related to the pressure parameter that maintains constant the total shear stress in the inner layer is used to define an eddy viscosity and diffusivity. The predicted velocity and temperature profiles agree reasonably well with the experiments. The essence of the formulation explains why the turbulent heat flux scaled by the local inner variables is merely unaffected contrarily to the Reynolds shear stress distribution in wall units that is significantly sensitive to the imposed pressure gradient.

1. Introduction

Turbulent boundary layers under the effect of adverse pressure gradient (APG) are an undergoing research topic since more than five decades. The first detailed investigation of turbulent APG flows is the well-known experimental work of Clauser [1] who studied equilibrium turbulent boundary layers with constant Clauser parameter β. To be globally self-similar, a turbulent boundary layer should experience a Falkner–Skan type of potential flow $\bar{u}_\infty \propto x^m$ and the turbulent length scale in the outer layer has to vary linearly with the streamwise distance x [2]. Subsequent experiments such as those conducted by [3] have clarified the statistical features and the fine structure of the turbulence in equilibrium APG flows. A few investigations based on direct numerical simulations restricted to low Reynolds numbers exist also in the literature by now [4]. Non-equilibrium APG turbulent boundary layers in which β is no more constant are less restrictive emerging from more general conditions. These flows have different characteristics merely in the outer layer that is not solely affected by local scales but is influenced by "historical" effects generated by downstream and upstream conditions [5–6]. Yet, there is a consensus by now that the inner layer in non-equilibrium APG turbulent layers is also managed by regional self-similarity induced by local parameters [7].

Turbulent transport of passive scalar has facets that are basically different from the transport of momentum in APG flows and the analogy between the heat and momentum transfer does no more hold. The temperature equation does not directly contain the pressure term, and the transfer process is indirectly affected by the pressure gradient through the eddy diffusivity. Yet, the thermal law of the wall is less robust than the velocity law of the wall [8–9] despite the fact that the Reynolds shear stress is strongly affected in the inner layer while the turbulent heat flux is insensitive to the APG [10].

There is a multitude of simple one-point closures concerning the turbulent boundary layers subjected to APG, such as for example the mixing length models derived from van Driest formulation [11,12]. The methodology followed in this note is somewhat different. The departure point is the determination of a local velocity scale already introduced by Skote and Henningson [13], which permits a local similarity formulation. We deduce an eddy viscosity and diffusivity by making use of this velocity scale that is directly related to the APG parameter. Analytic relations of velocity and temperature distribution are subsequently obtained in the inner layer and they are compared with recent experimental results of Houra and Nagano [10].

2. Local self-similar closure

The Reynolds averaged streamwise momentum equation in a two-dimensional turbulent boundary layer with pressure gradient reads for:

$$0 = -\frac{1}{\rho}\frac{d\bar{p}}{dx} + \nu\frac{\partial^2\bar{u}}{\partial y^2} - \frac{\partial}{\partial y}\overline{u'v'} \quad (1)$$

where the inertial terms have been locally neglected as usual. The total shear stress in wall units is obtained by integration of (1):

* Tel.: +33 476 827030; fax: +33 476 825271.
E-mail address: Sedat.Tardu@hmg.inpg.fr

0017-9310/$ - see front matter © 2008 Elsevier Ltd. All rights reserved.
doi:10.1016/j.ijheatmasstransfer.2008.11.019

Nomenclature

c_p	specific heat at constant pressure
k	conductivity
μ	dynamic viscosity
Pr	Prandtl number
Pr_t	turbulent Prandtl number
$\bar{q}_{tot}$	local total heat flux, $-\bar{q}_{tot} = k\frac{\partial \bar{T}}{\partial y} - \rho c_p \overline{v'T'}$
$\bar{q}_w$	mean heat flux at the wall
$\bar{p}$	mean pressure
$\bar{T}$	mean temperature
$\bar{T}_w$	mean wall temperature
$\bar{T}_\tau$	local friction temperature, $\bar{T}_\tau = \frac{\bar{q}_w}{\rho c_p \bar{u}_\tau}$
$\bar{\tau}_w$	mean wall shear stress, $\bar{\tau}_w = \rho \bar{u}_\tau^2$
$\bar{\tau}_{tot}$	total shear $\bar{\tau}_{tot} = \mu\frac{\partial \bar{u}}{\partial y} - \rho\overline{u'v'}$
$\bar{u}, \bar{v}$	mean streamwise and wall normal velocity components
u', v'	fluctuating streamwise and wall normal velocity components
$\bar{u}_\infty$	free-stream velocity
$\bar{u}_*$	turbulent velocity scale in the inner layer of APG flows, $\bar{u}_* = \bar{u}_\tau(1+\Pi^+ y^+)^{1/2}$
$\bar{u}_\tau$	shear velocity
x,y	streamwise and wall normal coordinates

Greek symbols

α_t	eddy diffusivity
β	Clauser parameter, $\beta = \frac{\delta_1}{\rho \bar{u}_\tau^2}\frac{d\bar{p}}{dx}$
δ	thickness of momentum boundary layer
δ_1	displacement thickness of momentum boundary layer
δ_c	thickness of conductive sublayer
δ_{mt}	edge of the fully turbulent mixing sublayer
δ_T	thickness of thermal boundary layer
$\bar{\theta}^+$	non-dimensional temperature, $\bar{\theta}^+ = \frac{\bar{T}_w - \bar{T}}{\bar{T}_\tau}$
ν	kinematic viscosity
ν_t	eddy viscosity
ρ	density
Π^+	pressure gradient parameter in local wall units, $\Pi^+ = \frac{1}{\bar{u}_\tau^3}\left(\frac{\nu}{\rho}\frac{d\bar{p}}{dx}\right)$

Subscripts and superscripts

$\overline{()}$	mean values
$()'$	fluctuating values
$()^+$	quantities normalized by the wall variables $(\nu, \bar{u}_\tau, \bar{T}_\tau)$

Abbreviations

APG	adverse pressure gradient
ZPG	zero pressure gradient

$$\bar{\tau}^+_{tot} = 1 + \frac{d\bar{p}^+}{dx^+} y^+ = 1 + \Pi^+ y^+ \tag{2}$$

where $()^+$ denotes quantities non-dimensionalized by the viscosity ν and the local shear velocity $\bar{u}_\tau(x)$ and:

$$\Pi^+ = \frac{1}{\bar{u}_\tau^3}\left(\frac{\nu}{\rho}\frac{d\bar{p}}{dx}\right) = \frac{1}{\bar{u}_\tau^3}\left(-\nu u_\infty \frac{du_\infty}{dx}\right) = \left(\frac{\bar{u}_\Pi}{\bar{u}_\tau}\right)^3 \tag{3}$$

is the non-dimensional pressure gradient parameter. In the viscous sublayer, the Reynolds shear stress is negligible. Therefore:

$$\bar{u}^+ = y^+ + \frac{1}{2}\Pi^+ y^{+2} \tag{4}$$

Eq. (2) indicates clearly that the shear velocity $\bar{u}_\tau(x)$ is not suitable for the self-similar formulation of the turbulent boundary layers with imposed pressure gradient. We consider the local velocity scale [13]:

$$\bar{u}_* = \bar{u}_\tau(1+\Pi^+ y^+)^{1/2} = \bar{u}_\tau\left(1 + \frac{\bar{u}_\Pi^3}{\bar{u}_\tau^3} y^+\right)^{1/2}$$

instead of $\bar{u}_\tau(x)$ that implicitly takes into account the pressure gradient. The total shear normalized by $\bar{u}_*$ becomes:

$$\bar{\tau}^*_{tot} = \frac{\bar{\tau}_{tot}}{\rho \bar{u}_*^2} = \frac{1}{\rho \bar{u}_*^2}\left(\rho\frac{\bar{u}_\Pi^3}{\bar{u}_\tau} y^+ + \rho \bar{u}_\tau^2\right) = 1 \tag{5}$$

in a way similar to canonical boundary layers in which $\bar{\tau}^+_{tot} = 1$. The velocity scale $\bar{u}_*$ directly intervenes in the formulation of the eddy viscosity $\nu_t \propto \ell_t u_t$ wherein ℓ_t and u_t are, respectively, the local turbulent length and velocity scales. Taking $u_t = \bar{u}_*$ instead of the local shear velocity, and $\ell_t = \kappa y$ as in canonical layers results in:

$$\nu_t = \kappa y \bar{u}_* = \kappa y \bar{u}_\tau (1+\Pi^+ y^+)^{1/2} \tag{6}$$

In the fully turbulent mixing sublayer, the viscous shear stress is negligible and:

$$\bar{\tau}_{tot} = \rho \bar{u}_*^2 = -\rho\overline{u'v'} = \rho \nu_t \frac{\partial \bar{u}}{\partial y} = \rho(\kappa y \bar{u}_*)\frac{\partial \bar{u}}{\partial y}$$

Inserting the definition of the modified velocity scale given by (3) in the last equation gives:

$$\frac{d\bar{u}^+}{dy^+} = \frac{\bar{u}^+_*}{\kappa y^+} = \frac{(1+\Pi^+ y^+)^{1/2}}{\kappa y^+} \tag{7}$$

in the fully turbulent mixing sublayer. The resulting velocity distribution reads for:

$$\bar{u}^+ = \frac{1}{\kappa}\left[\ln y^+ - 2\ln\left(\frac{\sqrt{1+\Pi^+ y^+}+1}{2}\right) + 2\left(\sqrt{1+\Pi^+ y^+} - 1\right)\right] + B(\Pi^+) \tag{8}$$

that is valid from the buffer to the edge of the fully turbulent mixing (log) layer. The coefficient $B(\Pi^+)$ is a function of the imposed pressure gradient as it will be discussed in detail later in this section. This result is not new, and has already been obtained by Skote and Henningson [13] who used a similarity form of the velocity gradient in the outer part instead of the eddy viscosity formulation given by (6).

There is no direct contribution of the pressure gradient to the temperature distribution that is indirectly affected in the constant flux region through the eddy diffusivity. The local temperature transport equation is:

$$0 = \alpha\frac{\partial^2 \bar{T}}{\partial y^2} - \frac{\partial \overline{v'T'}}{\partial y} \tag{9}$$

wherein the advection terms have been neglected as in (1). The total heat flux scaled with the inner variables is self-similar:

$$\bar{q}^+_{tot} = \frac{\bar{q}_{tot}}{\bar{q}_w} = \frac{\partial \bar{\theta}^+}{\partial y^+}\frac{\alpha + \alpha_t(y)}{\nu} = \frac{\partial \bar{\theta}^+}{\partial y^+}\left(\frac{1}{Pr} + \frac{1}{Pr_t}\nu_t^+(y^+)\right) = 1 \tag{10}$$

where $\bar{\theta}^+ = \frac{\bar{T}_w - \bar{T}}{\bar{T}_\tau}$ and $\bar{T}_\tau = \frac{\bar{q}_w}{\rho c_p \bar{u}_\tau}$. Thus, it is necessary to introduce a new velocity scale $\bar{u}_*$, to have self-similar velocity distribution, but the canonical wall variables $\bar{q}_w$ and $\bar{u}_\tau$ are just adequate for the self-similar formulation of the temperature distribution. In the conductive sublayer $y^+ \le \delta_c^+$ one simply obtains:

$$\bar{\theta}^+ = Pr\, y^+ \tag{11}$$

as in the turbulent boundary layer without adverse pressure gradient. In the fully turbulent sublayer wherein the molecular diffusion is negligible one has:

$$\frac{d\bar{\theta}^+}{dy^+} = \frac{Pr_t}{\nu_t^+} = \frac{Pr_t}{\kappa y^+ \bar{u}_*^+} = \frac{Pr_t}{\kappa y^+ (1 + \Pi^+ y^+)^{1/2}} \tag{12}$$

The temperature distribution is finally given by:

$$y^+ \le \delta_c^+ \quad \bar{\theta}^+ = Pr\, y^+$$

$$\delta_c^+ \le y^+ \le \delta_{mt}^+ \bar{\theta}^+ = Pr\delta_c^+ + \frac{Pr_t}{\kappa} \ln\left[\left(\frac{\sqrt{1+\Pi^+ y^+} - 1}{\sqrt{1+\Pi^+\delta_c^+} - 1}\right)\left(\frac{\sqrt{1+\Pi^+\delta_c^+} + 1}{\sqrt{1+\Pi^+ y^+} + 1}\right)\right] \tag{13}$$

wherein $\delta_c^+(Pr, \Pi^+)$ and δ_{mt}^+ denotes the edge of the fully turbulent mixing sublayer. It is supposed here that the turbulent Prandtl number is constant. The canonical relations are of course recovered as $\Pi^+ \to 0$.

3. Results

Fig. 1 compares the predicted velocity distribution given by Eqs. (4) and (8) with the relatively recent experimental results of Houra and Nagano [10]. The comparison is made with the strongest pressure gradient parameter $\Pi^+ = 2.56 \times 10^{-2}$ investigated by these authors for the sake of brevity. The Reynolds number based on the momentum thickness is $Re = 2730$ and the Clauser pressure gradient parameter is $\beta = 3.95$ in these experiments. Similar results have of course been obtained for smaller values of Π^+ reported by these authors. The best value of the constant appearing in Eq. (8) to fit the experimental data is $B(\Pi^+) = 2.5$ smaller than $B = 5$ of the zero pressure gradient (ZPG) turbulent boundary layer. The fact that the additive constant B depends on the adverse pressure gradient parameter and not the Reynolds number has already been clarified in [13]. For the stronger adverse pressure gradient $\Pi^+ = 6.90 \times 10^{-2}$ case that these authors have investigated through direct numerical simulations B has been set to $B = 1.5$, indicating that the additive constant decreases with Π^+. Fig. 1 shows that there is an excellent agreement between the model and the experiments in the inner layer $y^+ \le \frac{\delta^+}{2} \approx 300$. At $y^+ \ge \frac{\delta^+}{2}$, the wake component becomes significant. The outer layer in strong adverse pressure gradient (APG) flows is under the influence of historical effects that are hardly determined by local parameters [14]. The external zone is out of scope of this note.

Fig. 2 shows the temperature profile resulting from Eq. (13). The molecular Prandtl number is $Pr = 0.7$. The thickness of the conductive layer is set to $\delta_c^+ = 10$ to obtain the best fit to the experimental data. In the standard thermal layer one has $\delta_c^+ \approx 13$ at $Pr = 0.7$. It is

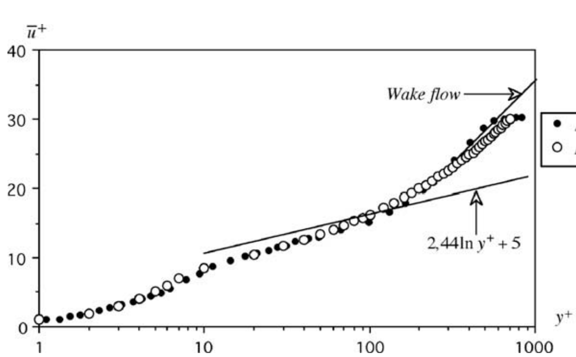

Fig. 1. Comparison between the velocity distribution given by the model (Eqs. (4) and (8)) and the experiments of Houra and Nagano [10] for $\Pi^+ = 2.56 \times 10^{-2}$. The flow configuration details are given in the text.

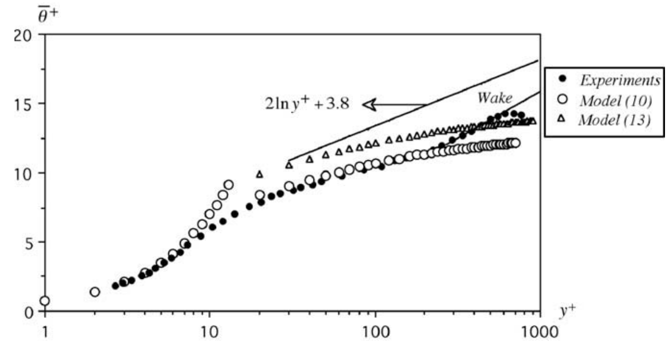

Fig. 2. Predicted temperature distribution in the inner layer compared with the experimental results of Houra and Nagano [10] for $\Pi^+ = 2.56 \times 10^{-2}$. The flow configuration details are given in the text. The triangles correspond to the conductive sublayer thickness $\delta_c^+ = 13$. Best fit is obtained with $\delta_c^+ = 10$ shown by the circles.

seen in Fig. 2 that $\delta_c^+ = 13$ results in an upward shift of the predicted values. Thus, the conductive sublayer thickness $\delta_c^+(Pr, \Pi^+)$ depends, yet slightly upon the imposed pressure gradient. The explanation of the differences observed in δ_c^+, in canonical and *APG* boundary layers is subtle. In two-layer approximate models of ZPG flows wherein the formulation of the buffer layer is omitted, the intersection of the linear $u^+ = y^+$ and logarithmic $u^+ = \frac{1}{\kappa}\ln y^+ + B$ velocity profiles takes place at $\delta_v^+ = 10.8$ (obtained by using $\kappa = 0.41$ and $B = 5$). In the presence of adverse pressure gradient, however the thickness of the diffusive layer δ_v^+ decreases. The intersection of Eqs. (4) and (8) yields indeed to $\delta_v^+ = 8.5$ that is 20% smaller than in the ZPG flow under the present conditions. Assuming as usual that $\frac{\delta_c^+}{\delta_v^+} \propto Pr^{-1/n}$ implies that the conductive sublayer thickness in APG flows decreases also in the same proportions. Using the values quoted to before gives indeed $\delta_c^+ = 10.3$ which is sensibly close to $\delta_c^+ = 10$ that fits the experimental data. Thus, one can estimate the thickness of the conductive sublayer in this simplified two-layer model quite easily, through the thickness of the diffusive velocity layer itself. More elaborated schemes have undoubtedly to take into account the dynamic and thermal buffer (transition) layers.

The turbulent Prandtl number is $Pr_t = 0.85$, thus unaffected by dP/dx in the inner layer, accordingly to [10]. The two-layer model reproduces nicely the experimental temperature distribution at $y^+ \le \frac{\delta_T^+}{2}$. The contribution of the (thermal) wake component to $\bar{\theta}^+$ in the outer layer is significantly larger than in the velocity distribution. The comparison of Figs. 1 and 2 shows the strong dissimilarity between the velocity and temperature distributions in the inner layer. Straight lines in these figures show the standard logarithmic laws of the zero pressure gradient turbulent boundary layers. It is seen that there is a systematic deficit in temperature distribution under the effect of adverse pressure gradient with respect to $\bar{\theta}^+ = 2\ln y^+ + 3.8$ of the canonical flow. The velocity distribution however is smaller and larger than the standard $\bar{u}^+ = 2.44\ln y^+ + 5$ law in, respectively, low and high log layers. The break-up of the temperature and velocity analogy results from the differences in the reaction to Π^+ of the Reynolds shear stress and wall normal turbulent heat fluxes. Indeed the Reynolds shear stress in local wall units contains directly the effect of the pressure gradient according to Eqs. (6) and (7), i.e.:

$$-\overline{u'v'}^+ = \frac{-\overline{u'v'}}{\bar{u}_\tau^2} = \nu_t^+ \frac{d\bar{u}^+}{dy^+} = 1 + \Pi^+ y^+ \tag{14}$$

In return, the wall normal turbulent heat flux scaled by the local wall variables, is unaffected by the adverse pressure gradient according to the self-similar formulation (10), and one has:

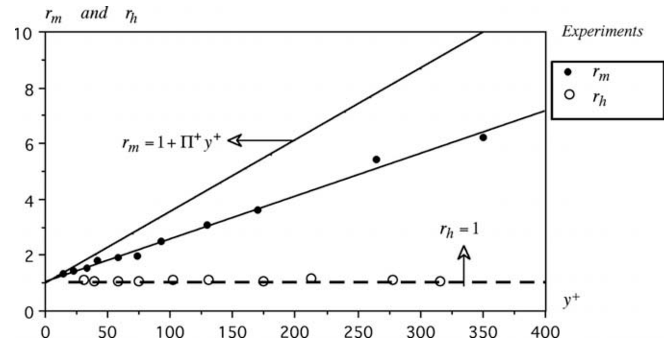

Fig. 3. Ratios of the Reynolds shear stress and turbulent heat flux to their respective values in the ZPG turbulent layer versus y^+. Comparison of the model is made with the experimental distributions [10] for $\Pi^+ = 2.56 \times 10^{-2}$.

$$-\overline{v'\theta'}^{+} = \frac{-\overline{v'\theta'}}{\bar{u}_\tau \bar{T}_\tau} = 1 \tag{15}$$

in the fully turbulent layer, exactly as in canonical turbulent flows. This is in agreement with [10] who indicated that the turbulent heat flux is unaffected by the adverse pressure gradient. Fig. 3 shows the quantities:

$$r_m = \frac{(-\overline{u'v'}^{+})_{\Pi^+}}{(-\overline{u'v'}^{+})_0}, \qquad r_h = \frac{(-\overline{v'\theta'}^{+})_{\Pi^+}}{(-\overline{v'\theta'}^{+})_0} \tag{16}$$

that are the ratios of the Reynolds shear stresses and heat fluxes in the APG and ZPG flows. The predicted values are obviously $r_m = 1 + \Pi^+ y^+$ and $r_h = 1$. There is a good qualitative and acceptable quantitative agreement between the predictions and the experiments. Fig. 3 shows that the experimental r_h values, collapse perfectly well with the theoretical $r_h = 1$ distribution but that the ratio r_m is over estimated. The experimental r_m distribution is linear as predicted by the model, with slop $\Pi^+ = 1.7 \times 10^{-2}$ that is 30% smaller than $\Pi^+ = 2.56 \times 10^{-2}$. This discrepancy may only partly be attributed to the experimental errors, yet the agreement is satisfactory taking into account the crudeness of the model investigated here. It is also asked here whether the real persistent parameter is the local Π or an effective pressure Π_{eff} that takes into account the upstream historical effects. The upstream mean pressure gradient in [10] is indeed $\Pi^+_{eff} = \frac{1}{x}\int_0^x \Pi^+(x)dx = 1.8 \times 10^{-2}$ which is curiously quite close to the experimental data slop in Fig. 3. That might be coincidental of course, and more detailed investigation is needed to confirm or reject this hypothesis.

4. Conclusion

To conclude, self-similar formulation introduced in [13] has been extended to the passive scalar transfer process in turbulent boundary layers in the range going from mild to strong adverse pressure gradients. There are acceptable concordances between the velocity and temperature distributions inferred from the two-layer closures introduced here and some recent experimental results. The Reynolds shear stress in APG scaled with the local $-\overline{u'v'}^{+}$ of the ZPG flow increases linearly in the inner layer as confirmed both by the model and the experiments. More over, the wall normal turbulent heat flux in wall units is unaffected by the adverse pressure gradient and the velocity and temperature distributions are entirely dissimilar. The proposed closure results in simple analytic velocity and temperature distributions in the inner layer that can be useful at least in a first exploratory stage of the flow analysis.

References

[1] F.H. Clauser, Turbulent boundary layers in adverse pressure gradients, J. Aero. Sci. 21 (1954) 91–108.
[2] A.A. Townsend, The Structure of Turbulent Shear Flows, Cambridge University Press, 1976.
[3] P.E. Skare, P.A. Krogstad, A turbulent equilibrium layer near separation, J. Fluid Mech. 272 (1994) 319–348.
[4] M. Skote, D.S. Henningson, R.A.W.M. Henkes, Direct numerical simulation of self-similar turbulent boundary layers in adverse pressure gradients, Flow Turbulence Combust. 60 (1998) 47–85.
[5] A.E. Samuel, P.N. Joubert, A boundary layer developing in an increasingly adverse pressure gradient, J. Fluid Mech. 66 (1974) 481–505.
[6] Y. Nagano, T. Tsuji, T. Houra, Structure of turbulent boundary layer subjected to adverse pressure gradient, Int. J. Heat Fluid Flow 19 (1998) 563–572.
[7] A.E. Perry, Turbulent boundary layers in decreasing adverse pressure gradients, J. Fluid Mech. 26 (1966) 481–506.
[8] P. Bradshaw, P.G. Huang, The law of the wall in turbulent flow, Proc. R. Soc. Lond. A 451 (1995) 165–188.
[9] R.J. Volino, T.W. Simon, Velocity and temperature profiles in turbulent boundary layer flows experiencing streamwise pressure gradient, Trans. ASME J. Heat Transfer 119 (1997) 433–439.
[10] T. Houra, Y. Nagano, Effects of adverse pressure gradient on heat transfer mechanism in thermal boundary layer, Int. J. Heat Fluid Flow 27 (2006) 967–976.
[11] T. Cebeci, P. Bradshaw, Physical and Computational Aspects of Convective Heat Transfer, Springer-Verlag, New York, 1988.
[12] D.C. Wilcox, Turbulence Modeling for CFD, second ed., Dcw Industries, 1998.
[13] M. Skote, D.S. Henningson, Direct numerical simulation of a separated turbulent boundary layer, J. Fluid Mech. 471 (2002) 107–136.
[14] A.E. Perry, W.H. Schofield, Mean velocity and shear stress distributions in turbulent boundary layers, Phys. Fluids 16 (1973) 2068–2074.